Hybrid Polymer Networks of Unsaturated Polyester–Urethane as Composite Matrices for Jute Reinforcement

B. Singh, M. Gupta, Anamika Randhawa, Simmi Tyagi, Sarika Sharma

Polymers, Plastics, and Composites Division, CSIR-Central Building Research Institute, Roorkee 247 667, India

Received 5 October 2010; accepted 28 January 2011
DOI 10.1002/app.34227
Published online 21 May 2011 in Wiley Online Library (wileyonlinelibrary.com).

ABSTRACT: Reactions of unsaturated polyester resin and 4,4′ diphenyl methane diisocyanate were carried out at different NCO/OH ratios in presence of catalysts to form the hybrid polymer networks. Chain extender (1,4 butanediol) added in the hybrid network (NCO/OH ratio: 0.76) was optimized at a level of ~ 3 wt % only of the polyester resin. The curing of these networks was studied by a rigid body pendulum type (RPT) method in terms of reduced damping ratio and increased frequency. Lack of multiple glass transition temperatures, sharp Tan delta peak, and particulate composite type morphology clearly demonstrated the formation of phase mixed domains in the hybrid networks. The storage modulus and loss modulus master curves obtained by dynamic mechanical analysis indicate that hybrid polymer networks retained higher modulus at lower and intermediate frequencies over the polyester resin showing their superior time-dependent response. Efficacy of these hybrid network resins was examined as matrices in the jute composites and compared with those of polyester resin and unsaturated polyester–polyurethane interpenetrating network matrices. It is found that the hybrid polymer network matrix composites exhibited superior physicomechanical properties under both dry and boiling water age test. Fractographic evidences such as fiber–matrix adhesion, hackle markings, and fiber breakage also supported their superior behavior over other composite matrices. © 2011 Wiley Periodicals, Inc. J Appl Polym Sci 122: 1206–1218, 2011

Key words: hybrid polymer network; composites; chain extender; AFM image; mechanical properties

INTRODUCTION

Fiber reinforced polyester composites find wide acceptance in the manufacture of a variety of building materials including panels, roofing sheets, doors and windows, and the like.[1–8] Typically, such composites are prone to micro-cracking and secondary bond failures (delamination) because of poor toughness and high volume shrinkage during curing process of the polyester resins.[4,9,10] Therefore, improvements in the physical and mechanical properties of polyester resin are highly desirable by making it tougher[11,12] and creating an optimum adhesion with the fibers.[13,14] In recent years, the hybrid polymer networks derived from unsaturated polyester and isocyanates have been recognized for this purpose to enhance the mechanical performance of the polyester resins.[15–19] It can be formed through the crosslink reactions, i.e., copolymerization of unsaturated polyester resin with styrene and polyaddition between terminal hydroxyl groups of polyester and isocyanate groups. The chemical bonds formed between both the resins can make their glass transition temperature too close and also make the effective damping temperature narrow, which will have the influence on the microstructure of hybrid polymer networks.[20] Adequate control of phase separation and interlocking of both polymer networks enhances the toughness and impact strength of hybrid networks.[21] Viewing these advantageous properties, it would be desirable to attempt such matrix resin with natural fiber reinforcement for the development of hydrothermally stable and tougher composites.

In the present study, we aimed at discussing an optimum stoichiometric NCO/OH ratio in the unsaturated polyester–urethane hybrid polymer network useful as matrix resin for jute composites and also sandwich core foamable compositions. It is expected that isocyanate terminated hybrid network reacts with the surface hydroxyl groups of jute fibers to form a chemical bond avoiding the known necessity of jute pretreatment with coupling agent,[14] coating,[22,23] alkali,[24,25] etc. mentioned in the prior art. As a consequence, improved mechanical properties of the jute composites are expected. Higher compatibility in both the resins can be achieved through the hybrid polymer networking rather than the interpenetrating technique because of chemical bonds formation. An additional advantage of the hybrid networks is that during cold mold pressing, manufacturing process of the composites shortens several times. Previously, attempts[26–28] have been made on the use of hybrid polymer network as a matrix resin for fiber reinforced composites. Yu et al.[26] studied the mechanical properties of carbon fiber reinforced

Correspondence to: Dr. B. Singh (singhb122000@yahoo.com).

polyester–urethane hybrid network with an isocyanate content of 20 wt % in the matrix. They reported that interlaminar shear strength of the composites was typically two to three times as high as that of the unsaturated polyester matrix composites. The failure mechanism in the composites made from low molecular weight polyester resin was mainly of fiber breakages, klinks, and transverse cracks. Gunduz et al.[27] have attempted to produce the glass fiber composites using polyester–isocyanate hybrid network at a NCO/OH ratio of 0.45. The tensile strength and toughness of these composites were improved when compared to the corresponding values of the unsaturated polyester matrix composites. Radenkov et al.[28] concluded the modification of glass fiber reinforced polyester with 2,4 toulene diisocyanate (8 wt %) during molding to obtain better properties than the conventionally used polyester resin. In previous work, attempts on producing jute composites with the hybrid polymer network as a composite matrix have not received much attention necessitating a thorough examination of their formulations and performance.

In this article, we report property optimization of unsaturated polyester–urethane networks as a function of NCO/OH ratio and chain extender content. The miscibility of constituent phases was examined by modulated differential scanning calorimetry, dynamic mechanical analysis, and atomic force microscopy. Jute composites made with the hybrid polymer networks were physicomechanically and fractographically characterized and compared them with the parent unsaturated polyester and polyester–polyurethane interpenetrating network matrix composites.

EXPERIMENTAL

Materials

Unsaturated polyester resin based on Isophthalic acid (viscosity, 650 cps; acid value, 16 mg KOH/g; hydroxyl value, 133 mg KOH/g; styrene, 35%) along with methyl ethyl ketone peroxide and cobalt naphthenate (6% cobalt content) was purchased from M/s Naptha Resins and Chemicals, Chennai (India). 4,4′ diphenyl methane diisocyanate (MDI-Empeyonate CR 100, NCO content, 31%; viscosity, 150 cps at 25°C) was received from M/s Huntsman International, Navi Mumbai (India). The 1,4 butanediol (Sigma-Aldrich) was used as a chain extender. Dibutyl tin dilaurate (Air Products, Allentown) and commercial grade sodium hydroxide were used as received. Nonwoven jute fabric (weight ~ 350 g m^{-2}) was procured from M/s Birla Corporation Ltd., Kolkata (India). Poly (vinyl acetate) emulsion mat forming grade was obtained from M/s Pidilite industries, Mumbai (India).

Preparation of samples

Unsaturated polyester–urethane hybrid polymer networks (HPN)

The unsaturated polyester resin was dehydrated under vacuum. Subsequently, it was blended with an isocyanate in a different stoichiometric NCO/OH ratio under nitrogen atmosphere. The blend was stirred for 5 min and accelerated by adding 1.2 wt % cobalt naphthenate and then drop by drop addition of 0.5% dibutyl tin dilaurate. The sample was then allowed to deaeration for 5 min. Methyl ethyl ketone peroxide (1.2 wt %) was then mixed in the resin composition immediately prior to molding and poured into a mold to cast 5-mm thick plate. The plate was cured for 24 h at room temperature followed by a postcuring for 4 h at 80°C. In another experiment, the hybrid polymer network was prepared by adding 1,4 butanediol to the unsaturated polyester resin prior to isocyanate addition and subsequently followed the above described procedure.

Unsaturated polyester–polyurethane interpenetrating polymer networks (IPN)

Polyurethane prepolymer was prepared by a thorough mixing of polyether polyol and isocyanate in a resin kettle at a molar ratio of 1 : 2 under nitrogen atmosphere at 50°C. The resulting prepolymer (~ 10 wt %) was blended with the unsaturated polyester resin containing cobalt naphthenate (0.4%). The prepolymer addition in the blend was optimized on the basis of a prerequisite workable viscosity required for the composite preparation. The blend was thoroughly agitated and degassed for 5 min. Thereafter, 1.2 wt % methyl ethyl ketone peroxide catalyst was added into it. The samples were cast on a brass mold to a thickness of 5 mm. The curing of these cast sheets was done at room temperature for 24 h and then postcured at 80°C for 4 h to complete crosslinking reaction.

Jute composite samples

Jute fabrics (weight: 350 g m^{-2}) were treated with 2 wt % aqueous sodium hydroxide solution to remove a waxy layer from their surfaces. These treated fabrics were sprayed with the mat forming grade poly (vinyl acetate) emulsion (8 wt % of fabrics), dried them to a harden state in an air circulated oven and then pressed under 1 MPa at 100°C for 2 min to obtain a molding grade mat. It is mentioned that the use of mat forming grade emulsion provides adequate resin wet-out to the jute fabrics after hot

compression and also reduced resin consumption in the laminates preparation. The mats were impregnated with different matrix resins such as unsaturated polyester, hybrid polymer networks, and interpenetrating network. Six impregnated mats were stacked, placed between two silicone paper lined brass plates and compressed it on a hydraulic press for 30 min at a pressure of 2 MPa. The demoulded samples (~ 50% jute content) were cured at room temperature for 24 h and then postcured at 80°C for 4 h under contact pressure.

Test methods

Rheology

The viscosity change during maturation of resins was measured by a stress controlled rheometer (Model Gemini, Bohlin Instruments) using 25-mm diameter parallel plate geometry with a 1-mm gap at a shear rate of 2/s at 25°C.

Rigid body pendulum type physical properties test (RPT)

A rigid body pendulum type testing machine (RPT-3000W, A and D Company, Japan) was used to study curing of the resin samples. The sample ($10 \times 40 \times 5$ mm^3) was fixed on the cooling and heating blocks and set the pendulum so that the knife edge, the fulcrum of the swing comes vertically into contact on the sample. The period of free vibration given to the pendulum was in the range of 0.05 to 2 s. The test temperature was kept between 25 and 225°C. By analyzing the vibration, logarithm damping ratio and frequency were obtained to assess a curing process. When the size of network was large, the pendulum moves a long distance to crush or stretch the network. Therefore, the period of time the pendulum swings increases. Contrary to this, when the size of network was small, the distance of pendulum movement shortens.

Modulated differential scanning calorimetry (MDSC)

Modulated differential scanning calorimetry (Model Q 2000 DSC, TA Instruments) of the samples equilibrated at −50°C was carried out between −40 and 200°C at a heating rate of 3°C min^{-1} under nitrogen atmosphere. Modulation with a ±0.8°C amplitude for a 40-s period was employed. A slow heating rate was selected to allow for a good deconvolution. The resultant reversing (heat capacity component) and nonreversing (kinetic component) signals of the samples were recorded.

Dynamic mechanical analysis (DMA)

Dynamic mechanical analysis (Model 2980, TA Instruments) of the samples was carried out under a single cantilever mode. The specimen of size $30 \times 13 \times 3$ mm^3 was mounted between the arms and a thermal run was recorded from 30 to 200°C at a heating rate of 5°C min^{-1} at 1 Hz. The storage modulus, loss modulus, and tan δ of the samples were recorded.

The frequency sweep measurement was also carried out in the temperature range of 40–110°C with 5°C increment for each step at frequency ranging from 1 to 100 Hz. Using time–temperature superposition software, each data set was shifted at a reference temperature of 80°C and master curves were constructed for storage modulus and loss modulus.

Atomic force microscopy (AFM)

Atomic force microscope (AFM-NTEGRA, NT-MDT) was used to measure the internal morphology of the resins. The sample of size $12.50 \times 8.0 \times 5.0$ mm^3 was mounted on a metal disk which was then held magnetically under the probe. A 100× microscope was used to view phase contrast in the samples under different magnifications.

Physical and mechanical tests

Density and water absorption of the jute composites were determined in accordance with ASTM D 570-05 and ASTM D 792-08, respectively. The tensile properties of samples were obtained according to ASTM D 638-08 with the use of a Hounsfield Material Testing Machine (H 25 KS) at a cross head speed of 5 mm min^{-1}. The flexural tests of samples were carried out as per ASTM D 790-02 at a cross head speed of 5 mm min^{-1} and span-to-depth ratio of 16 : 1. All results were the average value of five measurements.

Accelerated water resistance test

Accelerated water resistance test of the specimens was carried out by immersing them in the boiling water. The samples were subjected to immerse in the cold water and water was brought to the boiling. The samples were kept at boiling temperature for 2 h followed by its cooling in water. The aged samples were examined for dimensional changes and tensile properties.

Scanning electron microscopy (SEM)

Fractography of the aged and unaged tensile surfaces of the jute composites was performed on a scanning electron microscope (Model Leo 435). Prior to surface examination, fractured surfaces of the failed samples were vacuum coated with a thin film of Au/Pd to render them conductive.

TABLE I
Effect of NCO/OH Ratio on the Physical Properties of Unsaturated Polyester–Urethane Hybrid Networks

			Results of rigid body pendulum type physical properties testing equipment				
NCO/OH ratio	Viscosity at 25°C (Pas)	Gel time (min)	Peak transition point (°C)	Log. damping ratio	Distribution of network (M_w)	Size of network (n)	Hardness (s)
0	0.98	70	110	0.98	135 − 80 = 55	0.10	0.16
0.23	1.23	50	115	0.73	114 − 52 = 62	0.16	0.14
0.38	1.53	40	120	1.15	145 − 100 = 45	0.18	0.10
0.76	1.97	36	145	0.45	193 − 113 = 80	0.16	0.06
1.15	2.04	30	166	0.32	250 − 118 = 132	0.20	0.05
1.53	3.10	25	290	0.23	350 − 247 = 103	0.14	0.04

RESULTS AND DISCUSSION

Effect of NCO/OH ratio

The physical properties of unsaturated polyester–urethane hybrid networks at different NCO/OH ratio are given in Table I. It is observed that the maturation of resin reaches the saturation viscosity rapidly by adding MDI to the unsaturated polyester and increases further after thickening due to the conversion of end groups of unsaturated polyester resin into an isocyanate group to a maximum extent[29] (Fig. 1). Higher the concentration of MDI, the shorter the gelation time of the hybrid polymer networks. The workability of the resin was not affected when the amount of initiator was decreased, allowing enough time for the mixing operations necessary to manufacture a composite. The increase in viscosity of the hybrid polymer networks occurred few minutes after the addition of initiator. It is reported[28] that the nitrogen atom in the isocyanate group possesses an unshared electron pair by which it forms an unstable complex with the peroxide initiator. Therefore, decomposition rate of these radicals take place much quicker than that of the peroxide only.

The curing of hybrid polymer networks was assessed with the help of logarithmic damping ratio and the change of frequency (Fig. 2). By measuring the frequency (time of pendulum movement), the size of the network can be determined while the logarithmic damping ratio measures the viscosity change caused by a creation of the network. When isocyanate content increases in the polyester resin, the peak transition point in the curve was moved to the higher temperature sides while the logarithmic damping ratio was moved to the lower sides. It is noted that before reaching the peak transition point, the size of network in the resin was small and also main chain structure of the resin was too soft. As a

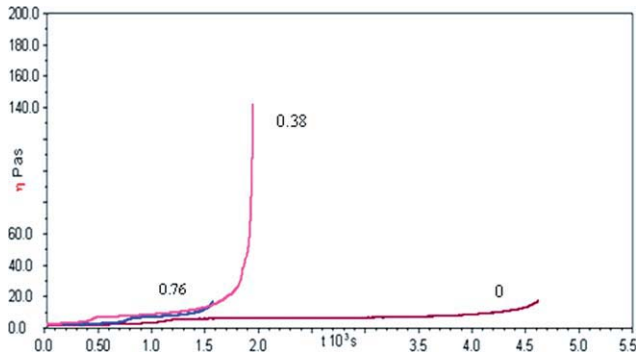

Figure 1 Viscosity versus time curves of unsaturated polyester resin at different NCO/OH ratio. [Color figure can be viewed in the online issue, which is available at wileyonlinelibrary.com.]

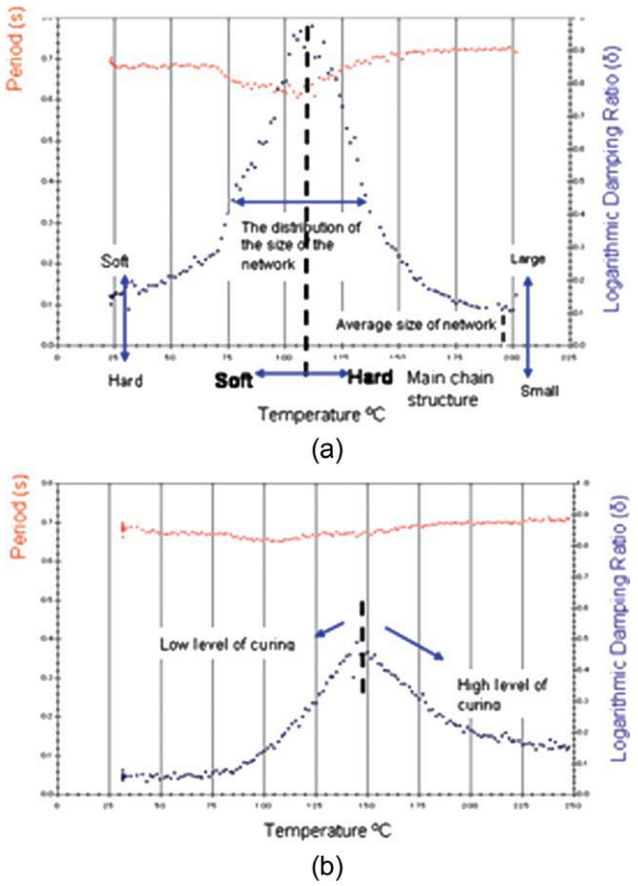

Figure 2 Rigid body pendulum type physical test (a) unsaturated polyester resin (b) hybrid polymer network (NCO/OH : 0.76). [Color figure can be viewed in the online issue, which is available at wileyonlinelibrary.com.]

TABLE II
Effect of NCO/OH Ratio on the Mechanical Properties of Unsaturated Polyester–Urethane Hybrid Networks

NCO/OH ratio	Tensile strength (MPa)	Elongation (%)	Tensile modulus (MPa)	Energy to break (J)	Flexural strength (MPa)	Flexural strain	Flexural modulus (MPa)	Impact strength (J m^{-1})
0	51.60 ± 2.60	4.72 ± 0.24	1376 ± 68.80	3.85 ± 0.19	53.67 ± 2.68	0.025	2190.61 ± 109.50	3.0 ± 0.15
0.23	55.19 ± 2.76	4.10 ± 0.21	1321 ± 66.05	3.98 ± 0.20	56.93 ± 2.85	0.020	2128.43 ± 106.40	8.0 ± 0.40
0.38	56.70 ± 2.84	5.78 ± 0.29	1209 ± 60.45	5.06 ± 0.25	69.98 ± 3.50	0.030	2332.67 ± 116.60	11.0 ± 0.55
0.76	70.70 ± 3.54	7.10 ± 0.36	1130 ± 56.50	7.81 ± 0.39	94.90 ± 4.75	0.043	2206.98 ± 110.35	15.20 ± 0.76
1.15	71.20 ± 3.56	7.26 ± 0.37	932 ± 46.60	7.51 ± 0.38	91.94 ± 4.60	0.051	1788.72 ± 89.40	13.0 ± 0.65
1.53	49.19 ± 2.46	4.80 ± 0.24	1463 ± 73.15	4.37 ± 0.22	70.24 ± 3.51	–	–	12.0 ± 0.60

result, damping ratio increases and consequently, the stickiness occurs in the samples. This indicates a level of low curing probably due to the movement of the physical networks. Above the peak transition point, the stickiness becomes small attributable to the creation and wider distribution of a large size networks following the temperature effects. It is noted that 10 wt % isocyanate addition to the unsaturated polyester resin (NCO/OH : 0.76) caused a significant reduction in the logarithmic damping ratio from 0.98 to 0.45 of the resulting system (Table I). The frequency of hybrid polymer networks was little affected with the temperature because of the formation of a large size network following the crosslinking. On the contrary, unsaturated polyester resin showed a clear shallow between 70 and 140°C in the frequency–temperature curve. After the peak point, the frequency increases with the increase of temperature and then leveled off due to cure effects. It is noted that surface hardness of the unsaturated polyester resin was lower than that of the hybrid polymer network when tested as per ISO 1522. The reduced logarithmic damping ratio and increased frequency favored a high level of curing in the hybrid polymer network compared to the unsaturated polyester.

As shown in Table II, the maximum tensile strength was reached at NCO/OH ratio of 0.76. As the isocyanate content reached at the optimum level, area under the tensile stress–strain curve (toughness) became larger showing an improvement of ~ 103% over the unsaturated polyester resin. Contrary to this, the tensile modulus of the hybrid polymer networks decreased by 17.80% at this level resulting from increased flexibility due to the presence of soft urethane domain.[15] The impact strength was also improved with the increase of isocyanate content at the optimum level. Beyond this level, excess of isocyanate may not contribute in the chain extension process and some polyester chains become NCO ended.[27,30] It is reported that the unreacted isocyanate remains in the resin also self catalyzed in the form of polyisocyanurate phase[31] and existed as a separate phase along with hard crosslinked polyester domain. As a consequence, the mechanical properties became poor and lead to the products with higher rigidity and worse impact.

Effect of chain extender

To enhance the toughness, chain extender was added to an optimized formulation of the hybrid polymer network (NCO/OH : 0.76). As shown in Table III, the tensile strength, elongation, and energy to break of the hybrid polymer networks increased and tensile modulus decreased as the chain extender was added up to a level of 3 wt % only. An increase of 25% in tensile strength and 45% in elongation were observed over the hybrid network without chain extender. Above this level, incorrect stoichiometric ratio between —OH group and —NCO group could result in a decrease in the mechanical properties due to low molecular weight of polyurethane.

TABLE III
Effect of Chain Extender on the Mechanical Properties of Unsaturated Polyester–Urethane

Chain extender content (%)	Tensile strength (MPa)	Elongation (%)	Tensile modulus (MPa)	Energy to break (J)	DMA tan δ peak (°C)	DSC T_g (°C)
0	70.70 ± 3.54	7.10 ± 0.36	1130 ± 56.50	7.81 ± 0.39	144	103.23
1	72.30 ± 3.62	8.26 ± 0.41	987 ± 49.40	8.42 ± 0.42	132	102.55
3	88.60 ± 4.40	10.27 ± 0.51	782 ± 39.10	11.46 ± 0.57	118	84.50
5	77.10 ± 3.86	9.48 ± 0.47	752 ± 37.60	9.63 ± 0.48	115	80.59
7	34.02 ± 1.70	3.54 ± 0.18	1233 ± 61.65	2.06 ± 0.11	102	63.66

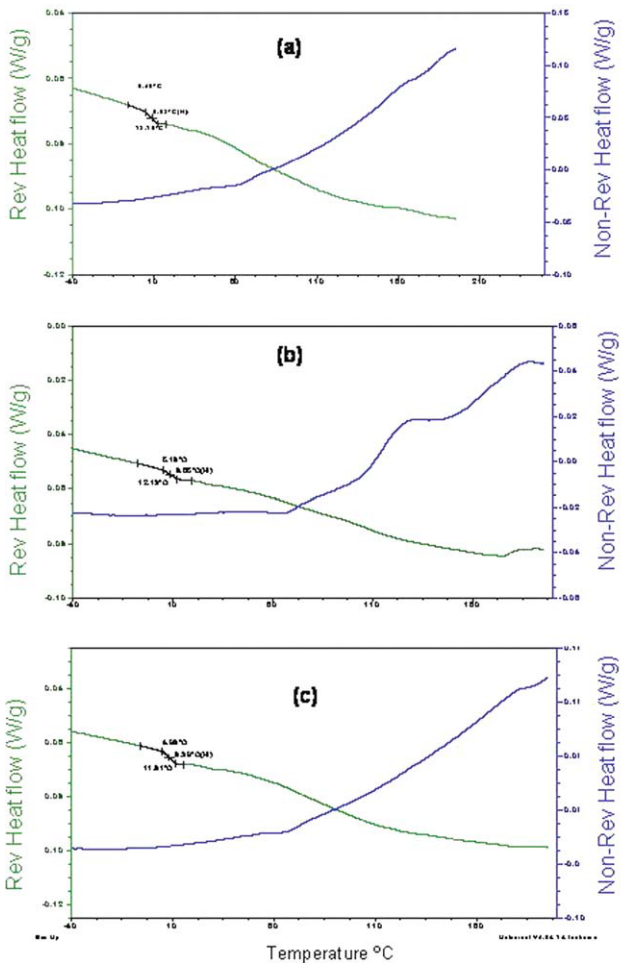

Figure 3 Modulated DSC traces (a) unsaturated polyester resin (b) hybrid polymer network (c) chain extended hybrid polymer network. [Color figure can be viewed in the online issue, which is available at wileyonlinelibrary.com.]

Residual chain extender may also play a role of plasticizer affecting the mechanical properties.[15]

Modulated DSC traces of the unsaturated polyester resin and its hybrid polymer networks are shown in Figure 3(a–c). It is noted that unsaturated polyester exhibited a transition at 8.82°C corresponding to the unpolymerized resin or peroxide crosslinked resin as reported earlier.[32] The broad nature of glass transition region as illustrated by reversible heat flow curve suggests that two types of network species: crosslinked polyester and polystyrene coexist (due to the low compatibility of styrene with polyester) as also evidenced in AFM images. As glass transition approaches the temperature at which curing occurs, the broad exotherm in the nonreversible curve obscured glass transition [Fig. 3(a)]. On the other hand, the hybrid polymer network displayed subtle glass transitions in the endothermic background corresponding to various phases [Fig. 3(b)]. The occurrence of reduced endothermic background compared to the parent polyester supportive of a high degree of intermixing of phases. This indicates that interlocking of phases occurs at the gel point reach, which restricts further phase separation.[21] In the reversible heat flow curve, crosslinking reaction initiates around 70°C. The presence of multiple cure exotherms in the hybrid network as against to parent polyester resin can be explained by its chain extension and crosslinking processes. When chain extender was added in the hybrid network, a broad step change was observed in the reversible base line curve of the resulting system and the transition temperature moves toward lower temperature with respect to that of the parent system [Fig. 3(c)]. Urethane has been linked to the unsaturated polyester resin chain structure which brings the soft characteristics of polyurethane into the rigid network structure.[15] The weight fraction of unsaturated polyester polyol in the resin mix decreased when more chain extender was added to the system. Since crosslinks come from the reaction between unsaturated polyester and styrene, a lower crosslinking density is expected with higher amount of chain extender.[16] As a result, increased rate of phase separation was occurred which affected the mechanical properties of the resulting systems.

AFM images of the hybrid polymer networks under semi phase contrast mode are shown in Figure 4(a–c). The morphology of unsaturated polyester resin appears to be granular, rigid, and heterogeneous in which both polyester and polystyrene coexist. The micro particle domains were emerged beyond the surface level. Under higher magnification, the black spherical particles of polystyrene were distributed throughout the microstructure [Fig. 4(a)]. The existence of heterogeneous morphology can be well correlated with a broad peak of tan δ obtained by DMA and broad endothermic background in MDSC. On the other hand, morphology of the hybrid polymer network was smooth, soft and particulate composite type in which urethane phase (dark area) was dispersed in the polyester matrix (bright area) [Fig. 4(b)]. Because of intermixing of phases, tan δ peak in the DMA was sharper and moves towards higher temperatures compared to the parent polyester resin. At higher magnification, larger phase domain size was viewed along with the occurrence of little phase separation. When chain extender was added to the hybrid polymer network, morphology appeared to be relatively more soft and homogeneous [Fig. 4(c)]. Under higher magnification, mat type microstructure was clearly visible. The phase contrast between the constituents was reduced due to the formation of polyester–urethane hybrid network phase as a continuous matrix. As a result, the tan δ peak of DMA was sharpened and moves towards lower temperatures due to dominant hybrid

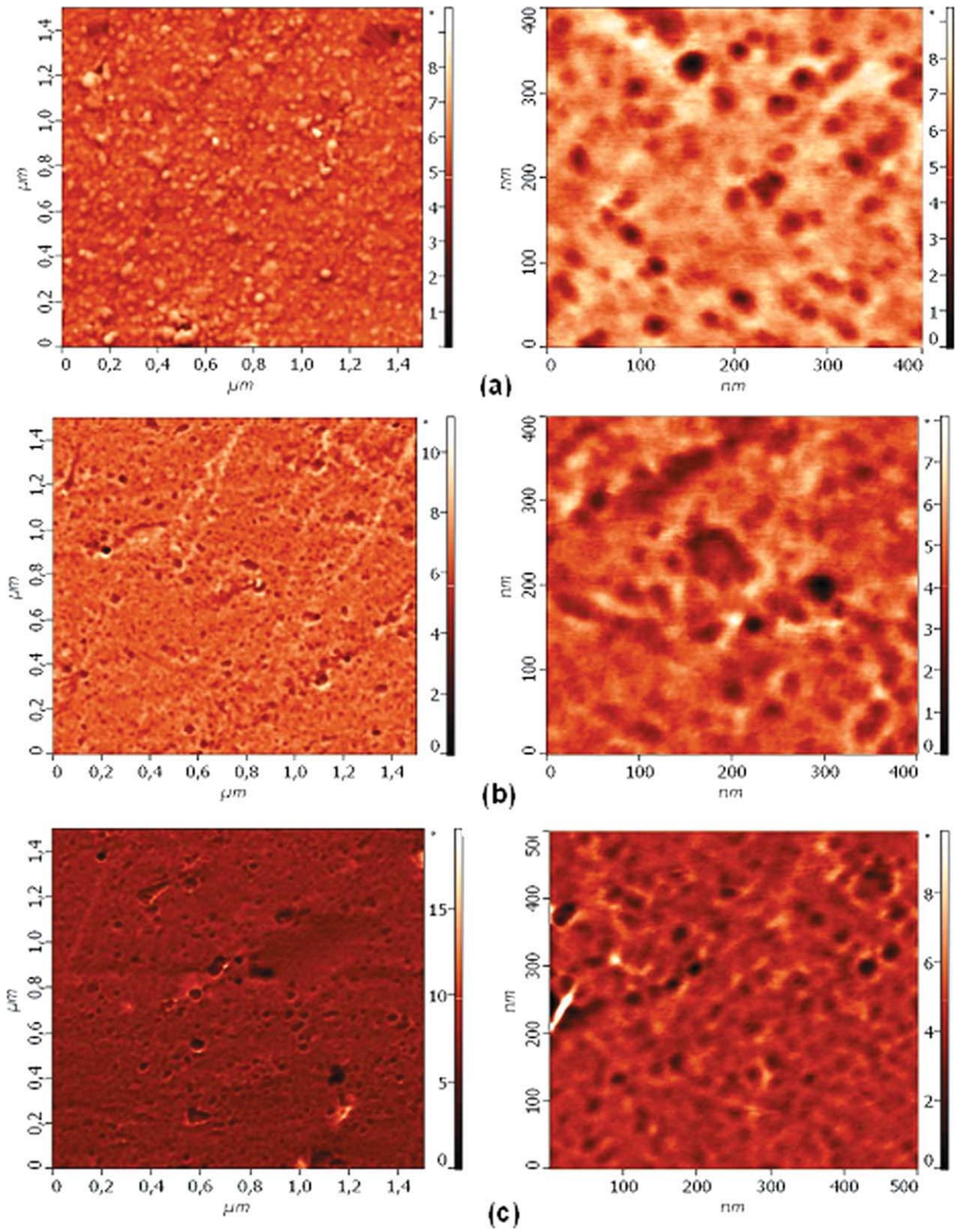

Figure 4 AFM images under semicontact phase contrast mode (a) unsaturated polyester resin (b) hybrid polymer network (c) chain extended hybrid polymer network. [Color figure can be viewed in the online issue, which is available at wileyonlinelibrary.com.]

network phase. The tan δ value was also higher than those of other systems showing its better damping characteristics (Fig. 5). It is noted that the hybrid polymer networks imparted higher modulus than the parent polyester resin over an entire range of temperatures.

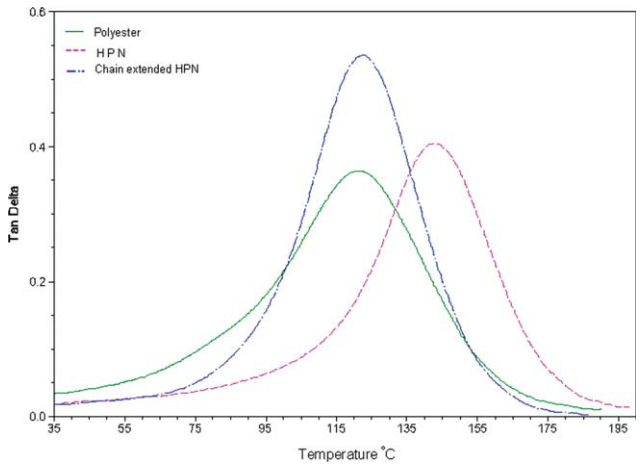

Figure 5 DMA traces: tan δ versus temperature of unsaturated polyester resin and hybrid polymer networks. [Color figure can be viewed in the online issue, which is available at wileyonlinelibrary.com.]

The dynamic mechanical properties of the hybrid polymer networks were studied by constructing master curves of storage modulus and loss modulus versus frequency at a reference temperature of 80°C (Fig. 6). The effect of time on the modulus of the samples was clearly demonstrated in the curves. It is noted that storage modulus of all the samples were almost the same at higher frequencies, whereas at lower frequencies, the hybrid polymer networks exhibited higher modulus values over the parent unsaturated polyester resin. These hybrid networks also present a large glassy plateau in the intermediate frequency region, which is due to the formation of molecular entanglement among the constituents. Because of a plateau, the slope in the curve was reduced and the samples exhibited little variations in the modulus values over the entire range of frequencies. The critical storage modulus of the hybrid network occurs at a frequency of 4×10^5 Hz as compared to 10^7 Hz for chain extended hybrid network and 10^6 Hz for parent polyester resin showing its better time dependent response. The loss modulus of the samples also changes with the varying frequencies. The effect of molecular network was clearly visible in the curve over a wide range of frequencies. It is observed that hybrid polymer network exhibited higher loss modulus than those of the other systems.

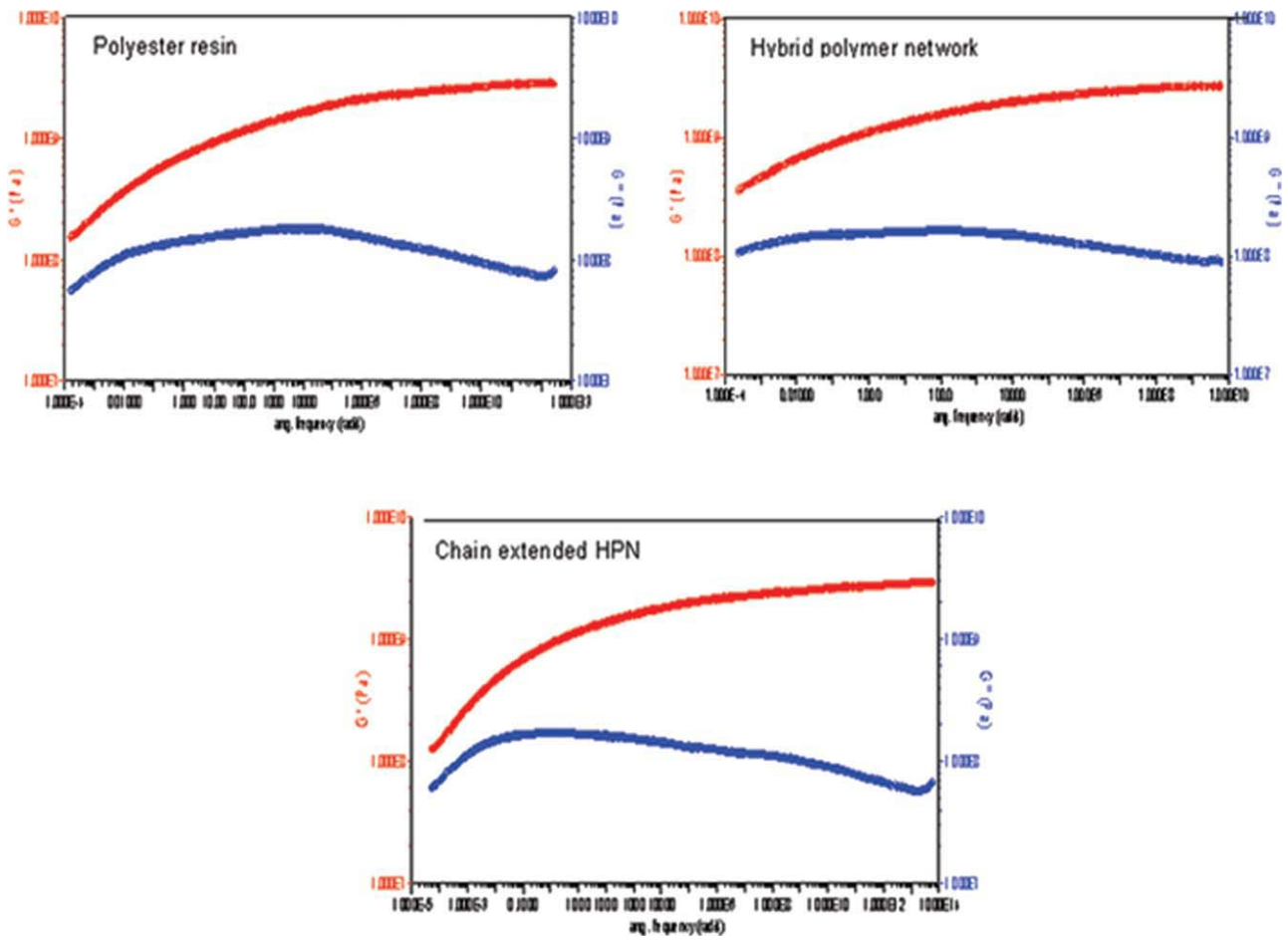

Figure 6 Storage modulus and loss modulus master curves of polyester resin and hybrid polymer networks at a reference temperature of 80°C. [Color figure can be viewed in the online issue, which is available at wileyonlinelibrary.com.]

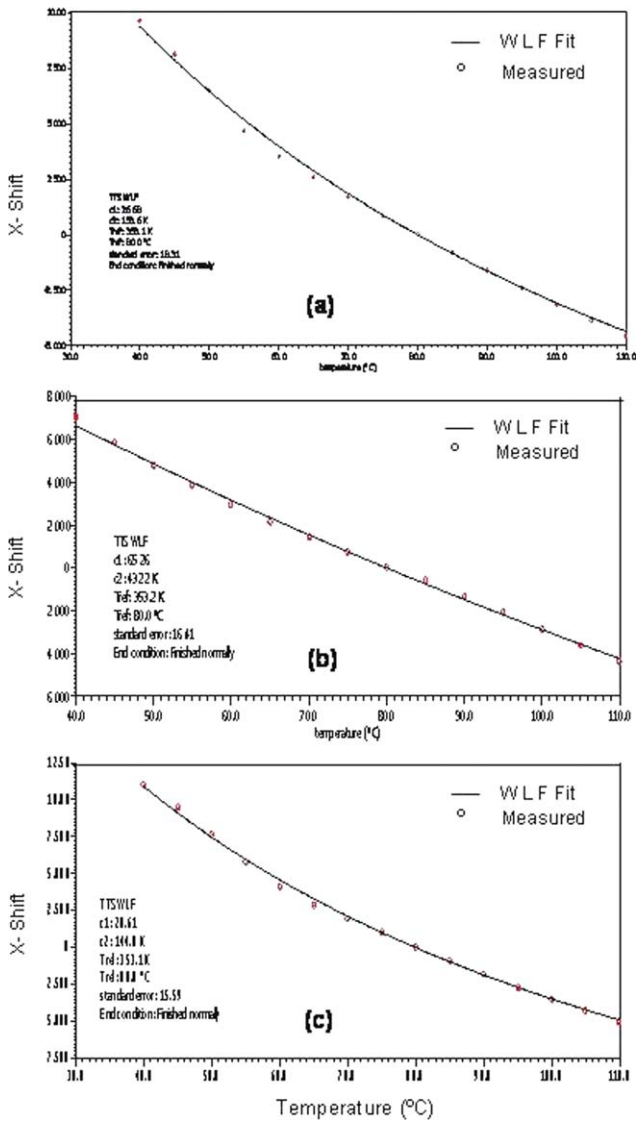

Figure 7 Plot of shift factor versus temperature (a) unsaturated polyester resin (b) hybrid polymer network (c) chain extended hybrid polymer network. [Color figure can be viewed in the online issue, which is available at wileyonlinelibrary.com.]

The shift factor plot obtained from the generation of the storage modulus master curve is displayed in Figure 7. Williams–Landel–Ferry equation (WLF)[33] was used to describe the time–temperature behavior of the hybrid polymer network at a reference temperature of 80°C.

$$\text{Log } a_T = \frac{C_1(T - T_0)}{C_2 + (T - T_0)}$$

where a_T is the shift factor measuring how a material's frequency response changes with the variation of temperatures; T, the temperature (K or °C); $T_{0,}$ the reference temperature (K or °C) and C_1 and C_2, the experimental material constants. It is noticed that there was an acceptable resemblance between theoretical and measured shifts above the glass transition temperature. The material constants C_1 (65.26 K) and C_2 (432.2 K) for the hybrid polymer network were significantly higher than the C_1 (26.68 K) and C_2 (153.6 K) of the parent unsaturated polyester resin. It is observed that the shift plot of the hybrid polymer network was less curved than the parent system showing its superior temperature resistance behavior. The hybrid polymer network incorporated with different percentage of chain extender exhibited variable material constants C_1 and C_2 in the range of 28.61–109.2K and 144.8–851.4 K, respectively. The activation energy of the shift factor calculated by the Arrhenius equation at a reference temperature of 80°C was 356.7 kJ mol^{-1} for the hybrid polymer network and 455.3 kJ mol^{-1} for the parent polyester resin. These activation energies are higher than those found in the literature.[16]

Composite properties

Performance of the hybrid polymer network was assessed as a matrix resin in the jute composites in terms of their physicomechanical properties and fractography (Table IV). Compared to the parent polyester matrix, the water absorption and thickness swelling of the HPN matrix composites were reduced by $\sim$ 36.82 and $\sim$ 66%, respectively after 24 h water immersion. An improvement of $\sim$ 23.48% in the tensile strength and 18.75% in the tensile modulus for HPN matrix composites was observed over the parent polyester matrix composites. The area under load-deflection curves was also increased by 16% only. It is due to the fact that the high adhesion between jute and hybrid polymer network resin may exist following the interaction between hydroxyl groups of jute and terminal isocyanate groups of polymer networks besides the formation of interpenetration between urethane and unsaturated polyester networks with chemical bond linking (Scheme 1). The possibility of interaction between jute and residual isocyanate in the matrix resin would also be existed. For comparison purpose, jute composites were also made with polyester–polyurethane IPN matrix. The tensile strength of HPN matrix composites was more than the IPN system whereas the water absorption and thickness swelling were less by 38.90 and 127.30%, respectively. It is believed that because of high molecular weight of IPN matrix, its wetting with jute fiber was inadequate to penetrate into the nonwoven jute fabrics. The increase in the elongation at break of IPN composite was attributed due to the predominant extensional deformation of networks and also the existence of slipping deformation between the networks. It is also noted that IPN

TABLE IV
Physico-Mechanical Properties of Jute Composites Using Various Network Resins

Property	Unsaturated polyester resin	Hybrid polymer network	Chain extended hybrid polymer network	Polyester–polyurethane network
Density (g cm^{-3})	1.20 ± 0.06	1.25 ± 0.06	1.19 ± 0.06	1.24 ± 0.06
Water absorption (%)				
2 h	1.85 ± 0.09	1.29 ± 0.06	1.14 ± 0.06	1.71 ± 0.09
24 h	6.28 ± 0.31	3.97 ± 0.19	3.60 ± 0.18	5.51 ± 0.28
Thickness swelling (%)				
2 h	1.98 ± 0.09	0.87 ± 0.04	0.45 ± 0.02	1.75 ± 0.09
24 h	4.61 ± 0.23	1.58 ± 0.08	1.32 ± 0.07	3.58 ± 0.18
Tensile strength (MPa)	57.50 ± 2.88	71 ± 3.55	71.20 ± 3.56	66.60 ± 3.30
Elongation at break (%)	5.86 ± 0.29	5.40 ± 0.27	6.12 ± 0.31	6.30 ± 0.32
Tensile Modulus (MPa)	1568 ± 78.40	1862 ± 93.10	1153 ± 57.65	1737 ± 86.90
Energy to Break (J)	4.16 ± 0.21	4.27 ± 0.21	5.01 ± 0.25	4.57 ± 0.23
Toughness (MPa)	25 ± 1.25	29 ± 1.45	34 ± 1.70	30 ± 1.50

matrix composites showed higher tensile strength and toughness than that of the polyester matrix composites. It is thought that polyurethane act as a bridging agent to increase the interaction between the jute and polyester by forming hydrogen bonds. Under 2-h boiling water aging test, the deterioration in the mechanical properties (tensile strength: 13–38%; tensile modulus: 27–54%) was noticed in all the samples (Fig. 8). When compared with the parent polyester, HPN matrix composites retained ~ 12%

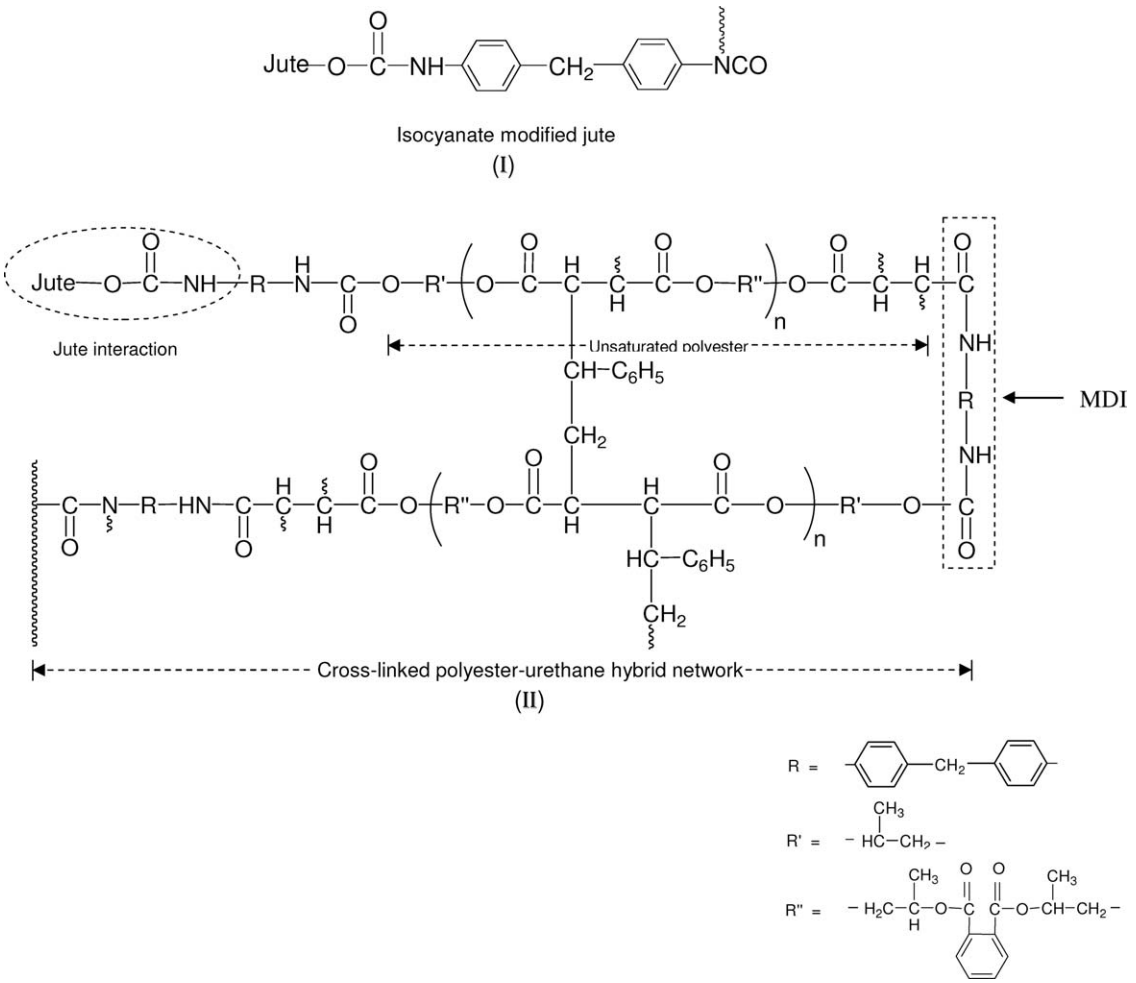

Scheme 1 Schematic representation of interaction between jute fiber and hybrid polymer network.

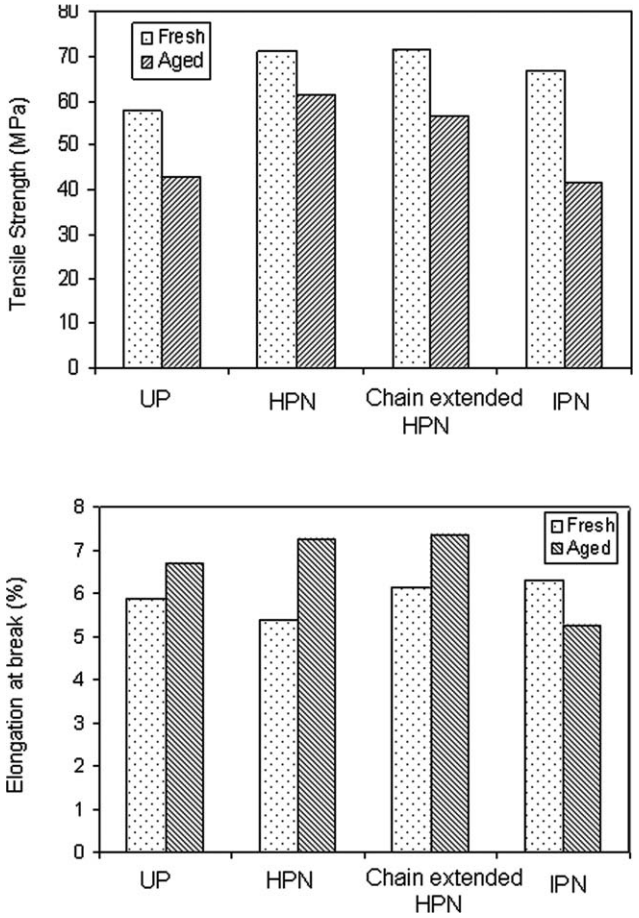

Figure 8 Tensile strength and elongation of fresh and aged jute composites using different resin matrices under 2-h boiling water.

more tensile strength while IPN matrix showed ~ 12% less tensile strength. The existence of superior hydrothermally stable bonds at the fiber–matrix interface in the HPN system could be responsible for such behavior. The elongation at break of aged samples increased (16.72–34.44%) probably due to debonding between jute fiber and resin.

The difference in the properties of the polyester matrix and HPN matrix jute composites can also be explained in terms of fracture surface morphology [Fig. 9(a–d)]. The tensile failure surfaces of the polyester matrix composites were characterized by the fiber pull-out, resin cracking and debonding between the fiber and resin [Fig. 9(a)]. It is noted that pulled-out fibers appears to be clean of any adhering resin suggesting interfacial failure. The increased fiber pulled-out was also indicative of weak shear strength of the polyester resin. The fractured surface was rough which was attributed to the fast crack propagation. On the other hand, fracture surface of the HPN matrix composites shows that most of the fibers were embedded along the fracture plane and well bonded to the matrix [Fig. 9(b)]. The presence of fracture line extending from the initiation site indicating the failure direction for that particular fiber. There was a distinct evidence of river patterns initiating from fiber-matrix boundary which suggest plastic flow of the resin. Hackle markings were seen in the matrix as evidence of shear yielding between the fibers and appear as more or less regular stacky of platelets. The formation of hackles was dominant feature for a tougher matrix. This is believed to be developed by microcracking in the matrix as the fracture surfaces peeled apart. The presence of mirror regions indicates flexibility in the matrix resin. In the case of chain extended HPN matrix composites, the matrix appeared to have undergone more ductile deformation and larger hackles formation between the fibers than the base HPN matrix composites [Fig. 9(c)]. The mirror regions were also dominant on the fracture surfaces which are indicative of slow crack propagation. In Figure 9(d), the facture surfaces of IPN matrix composites showed fiber pulled-out with resin adherence. Fine cracks due to cracking of the resin coating adhered on the fiber surface and locus of pulled-out fibers were also seen. While comparing the fractographic features of various composites, it is concluded that HPN matrix composites exhibited lesser extent of fiber pulled-out showing high shear strength, river markings at fibers leading to superior fiber–matrix interface, hackles formation contributing towards toughness of matrix and smooth surface attributed to slow crack propagation, which lead to the development of their superior mechanical properties.

CONCLUSIONS

Results indicate that the hybrid polymer networks at an optimized NCO/OH ratio exhibited larger network size, reduced logarithm damping ratio, and high mechanical strength than the parent polyester resin. The sharpened tan δ peak of DMA and mat type network morphology viewed in AFM provide the adequate evidences in support of intermixing of the two resins. Using time–temperature superposition principle, an acceptable fit between theoretical and measured shift factor was noticed above the glass transition temperature. Because of adequate fiber–matrix adhesion in the composites viewed in SEM, the hybrid network matrix escalates the possibility of pretreatment of jute fibers before their use in molding. The process of impregnating jute fabrics with this HPN matrix was also favorable because of its initial comparable viscosity to the polyester resin for thorough penetration in the fabrics. Jute composites made with HPN matrix showed a higher strength and toughness with additional improvement of the fracture behavior than the IPN and parent unsaturated polyester matrix composites under

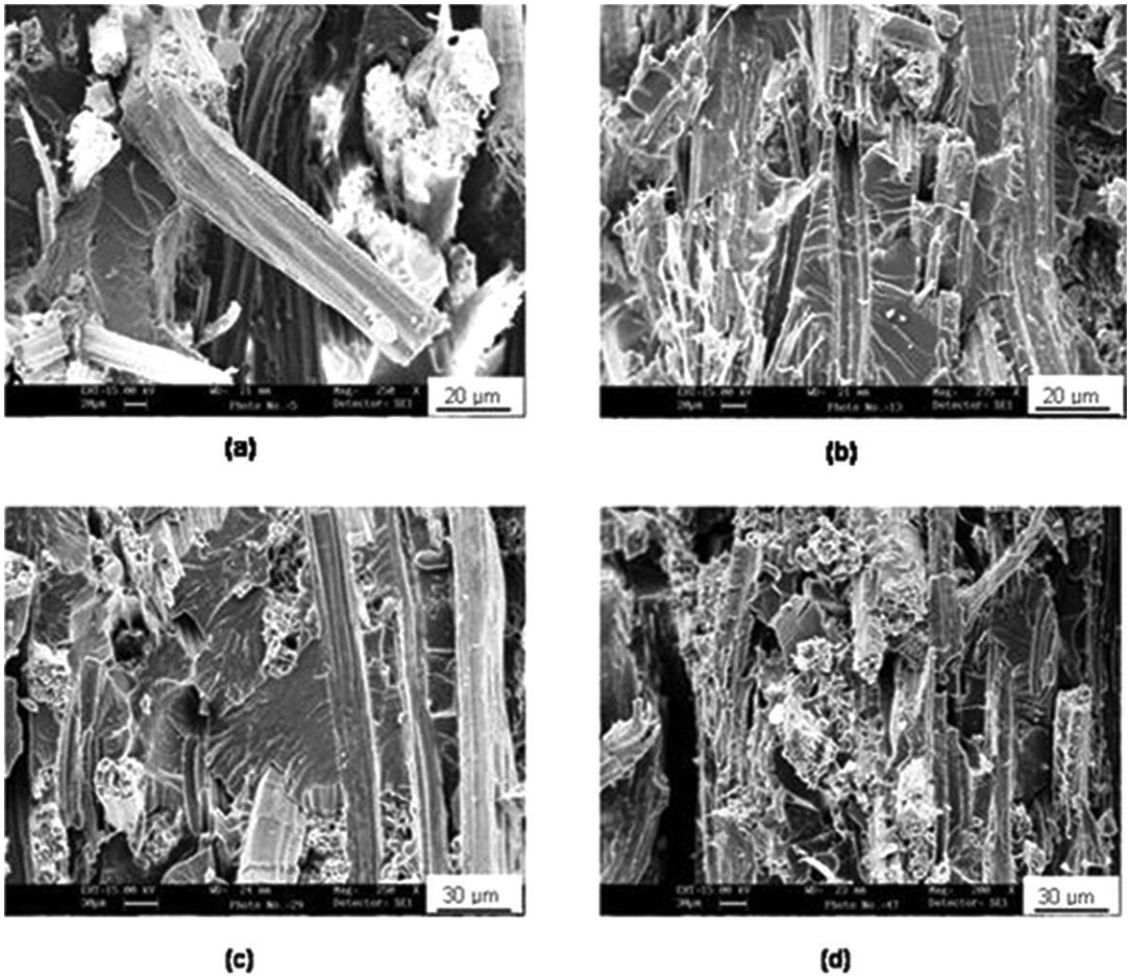

Figure 9 SEM of tensile fracture surface of jute composites using different resin matrices (a) polyester matrix composite (b) hybrid polymer networks matrix composite (c) chain extended hybrid polymer network matrix composite (d) unsaturated polyester–polyurethane IPN matrix composite.

both dry and wet conditions. Work is under progress on the performance of this network resin matrix under various kinds of moldings.

This article forms part of a Supra Institutional Project of CSIR R and D program (Govt. of India) and is published with the permission of Director, CSIR-Central Building Research Institute, Roorkee.

References

1. Winfield, A. G. Plast Rubber Intl 1979, 4, 23.
2. Belmares, H.; Barrera, A.; Castillo, E.; Verheugen, E.; Monjaras, M.; Paltfoort, G. A.; Bucquoye, E. N. Ind Eng Chem Prod Res Dev 1981, 20, 555.
3. Semsarzadeh, M. A. Polym Plast Technol Eng 1985, 24, 323.
4. Mitra, B. C.; Basak, R. K.; Sarkar, M. J Appl Polym Sci 1998, 67, 1093.
5. Mathur, V. K. Const Build Mater 2006, 20, 470.
6. Mohanty, A. K.; Misra, M.; Drazel, L. T., Eds. Natural Fibre, Biopolymers and Biocomposites; CRC Press: New York, 2005.
7. Singh, B.; Gupta, M. J Polym Environ 2005, 13, 127.
8. Singh, B.; Gupta, M.; Tarannum, H. J Bio Mater Bio Energy 2010, 4, 397.
9. Lin, S. P.; Shen, J. H.; Han, J. L.; Lee, Y. J.; Liao, K. H.; Yeh, J. T.; Chang, F. C.; Hsieh, K. H. Compos Sci Technol 2008, 68, 709.
10. Bryson, J. A. Plastic Materials; Butterworths Heinamann: Oxford, 1999.
11. Min, K. E.; Hwang, Y. G.; Choi, G. Y.; Kim, H. G.; Kim, W. S; Lee, D. H.; Park, L. S.; Seo, K. H.; Kang, I. K.; Jun, I. R.; Lim, J. C. J Appl Polym Sci 2002, 84, 735.
12. Wang, C.; Pan, Z.; Zhang, L.; Yang, D.; Li, W. Polym Adv Technol 2006, 17, 528.
13. Singh, B.; Verma, A.; Gupta, M. J Appl Polym Sci 1998, 70, 1847.
14. Xie, Y.; Hill, C. A. S.; Xiao, Z.; Militz, H.; Mai., C. Compos Part A 2010, 41, 806.
15. Hsieh, K. H.; Tsai, J. S.; Chang, K. W. J Mater Sci 1991, 26, 5877.
16. Valette, L.; Hsu, C. P. Polymer 1999, 40, 2059.
17. Xu, M. X.; Liu, W. G.; Guan, Y. L.; Bi, Z. P.; Yao, K. D. Polym Intl 1995, 38, 205.
18. Yang, Y. S.; Lee, L. J. Macromolecules 1987, 20, 1490.
19. Kim, J. H.; Kim, S. C. Polym Eng Sci 1987, 27, 1252.
20. Huang, G.; Li, Q.; Jiang, L. J Appl Polym Sci 2002, 85, 545.
21. Lee, D. S.; Kim, S. C. Macromolecules 1984, 17, 2193.
22. Varma, I. K.; Ananthakrishnan, S. R.; Krishnamoorthy, S. Composites 1989, 20, 383.

23. Mukherjee, R. N.; Pal, P. K.; Sanyal, S. K. J Appl Polym Sci 1983, 28, 3029.
24. Gasson, J.; Bledzki, A. K. Compos Sci Technol 1999, 59, 1303.
25. Sinha, E.; Rout, S. K. J Mater Sci 2008, 43, 2590.
26. Yu, J. L.; Liu, Y. M.; Jang, B. Z. Polym Compos 1994, 15, 488.
27. Gunduz, G.; Erol, D.; Akkas, N. J Compos Mater 2005, 39, 1577.
28. Radenkov, P. H.; Radenkov, M.; Dikov, V.; Lambov, S. Polym Bull 2006, 57, 91.
29. Chiu, Y. Y.; Saito, R.; Lee, L. J. Polymer 1996, 37, 2179.
30. Hepburn, C. Polyurethane Elastomers; Applied Science Publishers: England, 1982; Chapter 2, p 27.
31. Bukowski, A.; Gretkiewicz, J. J Appl Polym Sci 1982, 27, 1197.
32. Harpaz, I. M.; Narkis, M.; Siegmann, A. J Appl Polym Sci 2007, 105, 885.
33. Williams, M. L.; Landel, R. F.; Ferry, J. D. J Am Chem Soc 1955, 77, 3701.